

1 Potential effects of deep seawater discharge by an Ocean Thermal Energy Conversion 2 plant on the marine microorganisms in oligotrophic waters

3

4 **Mélanie Giraud^{1,2,3}, Véronique Garçon², Denis de la Broise¹, Stéphane L'Helguen¹, Joël Sudre², Marie Boye^{1,4}**

5 ¹LEMAR (UMR 6539), IUEM, Technopôle Brest-Iroise, 29280 Plouzané - France ; ²LEGOS (UMR 5566), 31401 Toulouse cedex 9 - France ; ³France
6 Energies Marines, 29200 Brest - France ; ⁴Present address : Institut de Physique du Globe de Paris (UMR 7154), 75005 Paris, France

7 Corresponding author: M. Boye (boye@ipgp.fr)

8

9

Abstract

10 Installation of an Ocean Thermal Energy Conversion pilot plant (OTEC) off the Caribbean coast of Martinique is
11 expected to use approximately 100 000 m³ h⁻¹ of deep seawater for its functioning. This study examined the potential
12 effects of the cold nutrient-rich deep seawater discharge on the phytoplankton community living in the surface warm
13 oligotrophic waters before the installation of the pilot plant. Numerical simulations of deep seawater upwelled by the
14 OTEC, showed that a 3.0 °C temperature change, considered as a critical threshold for temperature impact, was never
15 reached during an annual cycle on the top 150 m of the water column on two considered sections centered on the OTEC.
16 The thermal effect should be limited, less than 1 km² on the area exhibited a temperature difference of 0.3 °C (absolute
17 value), producing a negligible thermic impact on the phytoplankton assemblage. The impact on phytoplankton of the
18 resulting mixed deep and surface seawater was evaluated by *in situ* microcosm experiments. Two scenarios of water mix
19 ratio (2 % and 10 % of deep water) were tested at two incubation depths (deep chlorophyll-*a* maximum: DCM and bottom
20 of the euphotic layer: BEL). The larger impact was obtained at DCM for the highest deep seawater addition (10 %), with a
21 development of diatoms and haptophytes, whereas 2 % addition induced only a limited change of the phytoplankton
22 community (relatively higher *Prochlorococcus sp.* abundance, but without significant shift of the assemblage). This study
23 suggested that the OTEC plant would significantly modify the phytoplankton assemblage with a shift from pico-
24 phytoplankton toward micro-phytoplankton only in the case of a discharge affecting the DCM and would be restricted to a
25 local scale. Since the lower impact on the phytoplankton assemblage was obtained at BEL, this depth can be
26 recommended for the discharge of the deep seawater to exploit the OTEC plant.

27

28 **Keywords:** marine microbial ecosystem | biogeochemistry | modeling | artificial seawater discharge | *in situ*
29 experiments | environmental standards

30

31 **1. Introduction**

32 Ocean Thermal Energy Conversion (OTEC) uses the solar energy by exploiting the temperature gradient between
33 surface and bottom seawater. In an OTEC plant, the cold deep seawater pumped close to sea bottom is used to condense a
34 working fluid (like ammonia), whereas warm surface waters, pumped close to the surface, serve to evaporate it. The
35 difference of pressure, generated by the evaporation and condensation of the fluid, drives a turbine that produces
36 mechanical energy. This energy is then converted to electrical energy in a generator. Due to the need of a 20 °C difference
37 between the cold deep and the warm surface waters for the OTEC exploitation, tropical areas are well suited for the
38 installation of OTEC plants.

39 The Martinique, a tropical island of Lesser Antilles, is ideally suited for OTEC functioning with its narrow continental
40 slope in the Caribbean part of the island, allowing an implementation of the plant close to the coast. The implementation
41 of a 10 MW OTEC pilot plant off the Caribbean coast of Martinique is expected in 2020 as part of the french NEMO project
42 (Akuo Energy, DCNS). This OTEC will pump approximately 100 000 m³.h⁻¹ of deep seawater at 1100 m depth. In order to
43 optimize the energy efficiency, the deep seawater should be rejected close to the surface. However, this large discharge
44 could induce important disturbances on the upper ocean ecosystem, and this impact should be estimated.

45 Environmental assessment of OTEC functioning was studied since the 1980's (NOAA, 1981; 2010). The deep
46 seawater discharge was described as one of the major drivers impacting the marine environment in OTEC plant. However,
47 only a few studies specifically detailed this critical aspect (Taguchi et al., 1987; Rocheleau et al., 2012). The deep seawater
48 discharge in OTEC plant generates a phenomenon similar to the one naturally occurring in the ocean within upwelling
49 systems. Equatorward winds along the coast in the eastern Atlantic and Pacific linked to atmospheric high-pressure
50 systems force Ekman transport and pumping, relocating coastal surface waters offshore. Thereby, deep water transport
51 towards the surface is generated close to the coast. In these systems, the large amount of macronutrients and trace metals
52 carried to the euphotic zone by the enriched deep seawater supports a large development of the phytoplankton, making
53 upwelling the most productive oceanic regions (Bakun, 1990; Pauly and Christensen, 1995; Chavez and Toggweiler, 1995;
54 Carr and Kearns, 2003). By contrast, the tropical surface waters off the Caribbean coast of Martinique exhibit low nutrients
55 (nitrate and phosphate) concentrations (< 0.02 μmol.L⁻¹) and therefore, they can be significantly enriched by the deep
56 seawater discharge. Whereas phytoplankton assemblages in upwelling systems are usually dominated by large
57 phytoplankton and particularly by diatoms (Bruland et al., 2001; Van Oostende et al., 2015), the phytoplankton community
58 in oligotrophic systems is composed of smaller organisms (Agawin et al., 2000).

59 Due to these important differences in biogeochemical functioning and environmental microbiology, it is thus of
60 critical interest to investigate the potential effects of the deep seawater discharge of the planned OTEC plant on the
61 phytoplankton community off Martinique. Furthermore, it is crucial to provide a depth where the deep seawater could be
62 discharged without significant effect on the surface layer where phytoplankton is the most abundant. Indeed, no

63 environmental standards on the deep seawater discharge effects are available yet, while transitional blue energies such as
64 OTEC plants will likely expand in the near future.

65 In this study, the impact of deep seawater discharge on the thermal structure of surface waters was first assessed.
66 Modification of the surface waters stratification should indeed impact the phytoplankton community. A high-resolution
67 oceanic model was used to examine the thermal impact induced by the deep seawater dispersion. Eight configurations of
68 discharge depth were tested, corresponding to the deep chlorophyll-*a* maximum (DCM), the bottom of the euphotic layer
69 (BEL) and five depths below the BEL. Temperature differences between numerical simulations without and with the deep
70 seawater discharge were compared on the upper 150 m of a vertical section.

71 The distribution of the ambient phytoplankton community and the biogeochemical properties of the deep and
72 surface seawater mixture that could impact the phytoplankton community were then described. Phytoplankton
73 distribution and assemblage were detailed in order to assess short time and small scales variabilities of phytoplankton
74 assemblage and primary production in the study site.

75 Finally, in order to simulate the OTEC deep seawater input, enrichment experiments were conducted on the future
76 site of the pilot plant. Enrichment experiments are commonly used in oceanography to assess the effects on
77 phytoplankton community and primary production. For example, large iron (Fe) enrichment experiments were conducted
78 from 1993 to 2005 to estimate the potential of Fe limitation on ocean primary production (De Baar et al., 2005; Boyd et al.,
79 2007). Several experiments also showed that macro- and micro-nutrients enrichments induce changes in the
80 phytoplankton community in upwelling regions (Hutchins et al., 2002) as well as in oligotrophic regions (Kress et al., 2005).
81 Enrichment experiments were usually conducted with mesocosms immersed close to the surface (Escaravage et al., 1996;
82 Duarte et al., 2000) or in laboratory under artificial light and temperature using phytoplankton model species (Brzezinski,
83 1985). A laboratory experiment intended to evaluate the effects of an OTEC seawater discharge in Hawaiian waters on the
84 natural phytoplankton community was previously conducted (Taguchi et al., 1987) under such artificial conditions, and
85 thus, it could not totally reproduce what occurred in the natural environment. Other deep seawater discharge experiments
86 were realized *in situ* (Aure et al., 2007; Handå et al., 2014). For example, the use of a moored platform to upwell deep
87 seawater and discharge it close to the surface has shown an increase in primary production in a western Norwegian fjord
88 where the euphotic zone is nutrient-depleted during summer (Aure et al., 2007), as it would be expected with the OTEC
89 discharge in oligotrophic waters. Whereas such a pumping system is well adapted for pumping seawater at 30 m depth for
90 example, it cannot be applied for OTEC experiments where deep seawater must be collected far deeper (1100 m depth)
91 and also discharged more deeply in the water column to reduce the potential effects on the phytoplankton community.
92 These conditions can be obtained by the use of *in situ* microcosms, in which light and temperature are the same as in the
93 natural surrounding waters, avoiding additional bias, and several conditions (enrichment, incubation depth) can be
94 simulated. Therefore, we used the unique device of immersed microcosms we developed (Giraud et al., 2016) for assessing

95 the effects of deep seawater discharge on the phytoplankton community. Two incubation depths (DCM and BEL) with two
96 ratios of enriched seawater (mixtures of surface water with 2 % and 10 % of deep seawater) were tested.

97 These experiments allowed the evaluation of critical mixing rate and discharging depth where effect was maximal.

98 **2. Materials and methods**

99 **2.1. Modelling the thermal effect**

100 The hydrodynamic numerical model ROMS-Regional Ocean Model System (Shchepetkin and McWilliams, 2005;
101 2009) was used to describe the resulting thermal effect due to OTEC functioning. The model was run in a 2-ways AGRIF
102 configuration allowing to define a parent and child domains around the Martinique Island which are run simultaneously,
103 transferring automatically open boundary conditions. The parent grid ranges from 63° W to 59° W and 13° N to 15.9° N
104 with a resolution of 1/60° (around 1.8 km) while the child domain narrows the parent one and was from 61.74° W to 60.41°
105 W and 14.21° N to 15.11° N with a resolution down to 1/180° (around 600 m). The bottom topography and coastline are
106 interpolated from the GINA database (1/120°, www.gina.alaska.edu/data/gtopo-dem-bathymetry) (Fig. 1). The model is
107 forced by the monthly Climate Forecast System Reanalysis (NCEP-CFSR) for wind stress, heat and freshwater fluxes. For
108 the open boundary conditions and initial conditions of the parent domain, a monthly climatology computed from the
109 Simple Ocean Data Assimilation (SODA) reanalysis (Carton and Giese, 2008) was used for the dynamical variables
110 (temperature, salinity and velocity fields). The configurations were run without and with a deep seawater discharge
111 mimicking the OTEC functioning (Giraud, 2016). Eight cases of horizontal discharge settings were simulated at different
112 depths: i) the DCM (45 m), ii) the BEL (80 m), that were estimated on June 12th 2014, and 3) six depths below the euphotic
113 zone (110 m, 140 m, 170 m, 250 m, 350 m and 500 m). In the OTEC plant, deep water will be pumped at 1100 m where
114 temperature is around 5 °C and salinity 35. Circulation of this water through the plant system will warm it up until 8 °C prior
115 to its release in the upper ocean. We thus applied at the location of the OTEC plant (61°13'0" W, 14°35'48" N), a cold-water
116 discharge (temperature 8 °C, salinity 35) at a flow rate of 28 m³ s⁻¹ and with a northward orientation. The thermal impact of
117 the cold-water source was assessed documenting the differences between simulations without and with the modelled
118 OTEC plant functioning (Giraud, 2016).

119 **2.2. Field observations and *in situ* experiments**

120 **2.2.1. Sampling and analytical methods**

121 Temperature, salinity, and fluorescence profiles were performed on 12th, 13th, 18th and 19th of June 2014 using
122 Seabird SBE19+ probe with *in situ* Fluorimeter Chelsea AQUAtracka III.

123 Seawater was collected on 12th and 18th of June 2014 in the water column in ultra-clean conditions (Giraud et al.,
124 2016) to measure *in situ* parameters and to prepare the microcosms. Seawater and microcosms were sampled similarly in a
125 land laboratory a few hours after collection.

126 Nitrate (NO₃⁻), nitrite (NO₂⁻), phosphate (PO₄³⁻) and silicate (Si(OH)₄) concentrations were determined in filtered
127 waters (<0.6 µm; PC membrane) stored at -20 °C until analysis using a Bran + Luebbe AAIII auto-analyzer (Aminot and
128 K  rouel, 2007).

129 Filtered samples (0.2 µm; 300AC-Sartobran™ capsules) for dissolved trace metals determination were collected
130 under pure-N₂ pressure (0.7 atm) in acid cleaned low density polyethylene bottles, acidified with ultrapure HCl (pH < 2) and
131 stored in two plastic bags in dark at ambient temperature. Concentrations of dissolved trace metals (cadmium: Cd; lead:
132 Pb; iron: Fe; zinc: Zn; manganese: Mn; cobalt: Co; nickel: Ni; and copper: Cu) were determined in UV-digested samples by
133 ID-ICP-MS (Milne et al., 2010) after preconcentration on a WAKO resin (Kagaya et al., 2009) using an Element XR ICP-MS.
134 Blanks, limits of detection, accuracy and precision (assessed using reference samples) of the ID-ICP-MS method are
135 reported in Table 1. The values determined by ID-ICP-MS were in excellent agreement with the consensus values, apart for
136 Cd that yielded higher concentration in S-SAFE reference sample than the consensus value (Table 1).

137 The pH was determined using a pH ultra-electrode (pHC28) mounted on a HQ40d multi pH-meter (HACH) with an
138 accuracy of ± 0.002 pH unit in samples preserved with saturated HgCl₂ in glass bottles hermetically closed with Apiezon
139 grease, sealed with Parafilm® and stored in the dark at ambient temperature.

140 Three complementary methods were used to analyze the phytoplankton community. Pigment signatures were
141 measured by HPLC (using an Agilent Technologies 1100-series) on polysulfone filters (0.22 µm pore-size) frozen at -20 °C
142 and stored in liquid nitrogen, after internal standard addition (vitamin E acetate) and extraction in a 100 % methanol
143 solution (Hooker et al., 2012). Fifty pigments were identified and associated to phytoplankton groups (Uitz et al., 2010).
144 Identification and enumeration of pico-phytoplankton were realized by flow-cytometry using a BD-FACSVerse™ (Marie et
145 al., 1999) in samples preserved in cryotube with addition of 0.25 % glutaraldehyde frozen at -20 °C and stored in liquid
146 nitrogen. Four groups of pico-phytoplankton were identified: *Prochlorococcus*, picoeukaryotes (< 10 µm), and 2 groups of
147 *Synechococcus* discriminated, respectively, by their low and high phycourobilin (PUB) to phycoerythrobilin (PEB) ratios.
148 Taxonomic identification and enumeration of micro-phytoplankton (20-200 µm) and a part of nano-phytoplankton (2-20
149 µm) (Dussart, 1966) were carried out using an inverted microscope (Wild M40) in samples preserved with neutral lugol
150 solution. Uterm  hl settling chambers (Hasle, 1988) were used for micro-phytoplankton analyses, and a smaller
151 sedimentation chamber (2.97 mL) for the analyses of nano-phytoplankton. When possible, phytoplankton was identified
152 to the lowest possible taxonomic level (species, genus or group) using the classical manual for marine phytoplankton
153 identification (Thomas, 1996) and the World Register of Marine Species database (WoRMS Editorial Board, 2019).
154 Biovolume of each species was also estimated from these microscope analyses (Hillebrand et al., 1999).

155 2.2.2. *In situ* microcosm experiments

156 The potential impact of deep seawater discharge on the phytoplankton community was simulated by *in situ*
157 microcosm incubations of various deep and surface seawater mixing (Giraud et al., 2016). The experiments were

158 conducted from 12th (D0) to 19th (D7) of June 2014. The deep and surface seawaters were collected at the site of the future
159 OTEC pilot plant (61°11'52" W-14°37'57" N; Fig. 1). Microcosms bottles were incubated on two stainless steel structures set
160 at the depths of deep chlorophyll-*a* maximum (DCM) and at the bottom of the euphotic layer (BEL) on a mooring chain
161 located, for practical reasons, closer to the coast (61°10'9" W-14°39'8" N, seafloor at 220 m depth) during 6 days (Giraud et
162 al., 2016). This incubation time was chosen to represent the short-term phytoplankton response time to a mixing of deep
163 water with surface waters.

164 This duration is shorter or equal than the residence time of the enriched water mass, which is less than one month.

165 Seawater was collected at D0 at the depths of DCM (45 m depth) and BEL (80 m depth) identified on the future
166 OTEC site from the fluorescence profile, and close to the bottom (1100 m depth corresponding to the pumping depth of
167 the future OTEC plant) in ultra-clean conditions. Deep seawater was mixed in three proportions (0 % as a control hereafter
168 referred to as "Control", 2 % as a low input called "2 % of deep seawater", and 10 % as a large input called "10 % of deep
169 seawater") with DCM and BEL waters. Each resulting mixture was distributed in 2.3 L polycarbonate bottles filled up to
170 overflow level, of which four replicates per mixing condition per depth were immersed at their respective sampling-depth
171 for 6 days; duplicates per mixing condition per depth were kept in dark at 25 °C for a few hours until sampling for later
172 characterization of phytoplankton assemblage and biogeochemical properties at D0 (called "Surrounding waters D0"); and
173 duplicates per mixing condition per depth were used to estimate carbon and NO₃⁻ uptakes at D0 (called "Surrounding
174 waters D0") as described below.

175 Same sampling and mixtures were realized at day 6 (D6, June 18th) just to evaluate the temporal evolution in the
176 natural environment, resting on duplicate bottles per mixing condition per depth for phytoplankton and biogeochemical
177 characterizations at D6 (called "Surrounding waters D6") and using other duplicates to estimate carbon and NO₃⁻ uptakes
178 at D6 (called "Surrounding waters D6").

179 After the 6 days incubation, all the incubated microcosm bottles on the mooring (called "Microcosm D6") were brought
180 on board. A quarter of each four replicates per condition was put in a new 2.3 L clean bottle and used to estimate carbon
181 and NO₃⁻ uptakes after 6 days of incubation (called "Microcosm D6"). The remaining microcosm contents were kept for
182 sampling and analysis.

183 2.2.3. Carbon and nitrate uptakes

184 Carbon (primary production) and NO₃⁻ uptake rates were estimated in the same sample using the dual ¹³C/¹⁵N
185 isotopic label technique (Slawyk et al., 1977). Immediately after sampling, ¹³C tracer (NaH¹³CO₃, 99 atom%, Eurisotop, 0.25
186 mmol¹³C.mL⁻¹) and ¹⁵N tracer (Na¹⁵NO₃, 99 atom%, Eurisotop, 1 μmol¹⁵N.mL⁻¹) were added to seawater mixtures at 10⁻³:1
187 v/v ratio. The initial enrichment was 10 atom% excess of ¹³C for the bicarbonate pool and 16-95 atom% excess of ¹⁵N for
188 the NO₃⁻ pool depending on the ambient NO₃⁻ concentration. The ¹³C/¹⁵N amended bottles were incubated for 24 h on the
189 mooring line at the DCM and BEL depths, after which 1 L samples were filtered onto pre-combusted (450 °C, 4 h) glass

190 fiber filters (Whatman). Filters were stored at -20 °C and oven dried (60 °C, 24 h) prior to analysis. Concentrations of
191 carbon (POC), nitrogen (PON) as well as ¹³C and ¹⁵N enrichments in particulate matter were measured with a mass
192 spectrometer (Delta plus, ThermoFisher Scientific) coupled to a C/N analyzer (Flash EA, ThermoFisher Scientific).
193 Standard deviations were 0.009 μM and 0.004 μM for POC and PON, and 0.0002 atom% and 0.0001 atom% for ¹³C- and
194 ¹⁵N-enrichments, respectively.

195 The absolute uptake rates (ρ , in $\mu\text{mol}\cdot\text{L}^{-1}\cdot\text{h}^{-1}$) were calculated for nitrogen (Dugdale and Wilkerson, 1986) and carbon
196 (Fernández et al., 2005) using the particulate organic concentrations measured after 24 h of incubation. These rates were
197 converted into biomass specific uptake rates (V_C or $V_{\text{NO}_3^-}$, in $\mu\text{mol}\cdot(\mu\text{g Chl } a)^{-1}\cdot\text{h}^{-1}$) by dividing ρ by the total chlorophyll *a*
198 concentration (TChl *a* defined as the sum of chlorophyll *a* and divinyl chlorophyll *a*) measured at the end of the
199 incubations. The addition of ¹⁵N tracer would cause a substantial increase in dissolved inorganic nitrogen concentrations
200 especially in the surface waters and, in turn, an overestimation of uptake rates (Dugdale and Wilkerson, 1986; Harrison et
201 al., 1996). The NO_3^- uptake rates were corrected for this perturbation (Dugdale and Wilkerson, 1986) using a half-
202 saturation constant of 0.05 $\mu\text{mol}\cdot\text{L}^{-1}$ characteristic for nitrogen-poor oceanic waters (Harrison et al., 1996) and the
203 measured NO_3^- concentration. Overestimation was low (< 5 %) in samples with an addition of deep seawater but it was of
204 about 50 % in samples without deep seawater addition. The uptake rates measured in these samples represented
205 therefore estimations rather than actual values.

206 2.2.4. Statistical analyses

207 Kruskal-Wallis test was applied on the set of pigments concentrations, pico-phytoplankton abundances and
208 macronutrients concentrations. If significant differences ($p < 0.05$) were found, Mann-Whitney test was run to identify the
209 samples significantly different. Statistical analyses were performed using Statgraphics Centurion XVI software.

210 3. Results

211 3.1. Impact of the deep seawater discharge on the thermal and density structure in surface

212 The representation of the thermocline and halocline depths, key proxies for oceanic mixing and for estimating the
213 thermal impact of the OTEC discharge, is well mimicked over the 2 months (June and November) of the mesocosm
214 experiments (Giraud, 2016). In order to assess the deep seawater discharge impact on the thermal structure of the upper
215 150 m of the water column, the dispersion of temperature differences (ΔT in °C) obtained without and with the deep
216 seawater discharge in the model outputs was examined on two vertical sections. A section of 124 km for the large domain
217 (corresponding to the child domain) and another section of 10 km for the near-OTEC domain (defined from 61.24° W to
218 61.17° W and 14.60° N to 14.67° N) were defined, both centered on the OTEC site and parallel to the coast (Fig. 1).

219 Presently, there are no environmental standards defining threshold levels for temperature difference that will be
220 induced by an OTEC deep seawater discharge. So, the study relied on the World Bank Group prescriptions for liquefied

221 natural gas facilities which set at 3 °C the temperature difference limit at the edges of the zone where initial mixing and
222 dilution take place (IFC, 2007). We thus considered for each discharge depth the cooling and warming outputs from the
223 model, which exhibit a $|\Delta T| \geq 3$ °C. Areas (in % of the considered domain) impacted by these cooling and warming effects
224 were added (absolute values) in order to compare the potential impact of each discharge depth configuration. None of the
225 discharge depth configurations could produce a modification of the thermal structure of the top 150 m of the water
226 column, higher than or equal to the considered temperature threshold ($|\Delta T| \geq 3$ °C), for both domain sections.

227 Then, a lower temperature difference of 0.3 °C (absolute value) was considered. This temperature difference
228 represented a low threshold as compared to the World Bank Group prescriptions (IFC, 2007) that instead represent a high
229 threshold. The areas exhibiting a $|\Delta T| \geq 0.3$ °C in the top 150 m (Table 2) were extremely small (< 1 km²) and were not
230 significantly different in both sections and at the different discharge depths, on an annual average and in June (our
231 experimental period).

232 We also investigated the OTEC impact on density. The density of water being discharged at 45 m, depth of the deep
233 chlorophyll maximum (DCM), is 27.48 (8°C and salinity of 35). The density of water at 45 m is around 23.72 (temperature of
234 28°C and salinity of 36.5) so the nominal density gradient is of 3.76. If one considers a modification of the density structure
235 of the top 150 m of the water column of $|\Delta \rho| \geq 0.1$, there is no impact when the discharge occurs at the depth of the DCM. If
236 one considers a lower density difference of 0.05 (absolute value), the area exhibiting a $|\Delta \rho| \geq 0.05$ in the top 150 m is
237 extremely small (< 1.5 km²) in both sections at the depth of the chlorophyll maximum. As far as we know, there are no
238 environmental standards defining threshold levels for density difference that will be induced by an OTEC deep seawater
239 discharge. This represents less than 1.5 % of the nominal density gradient so as for the thermal impact, the impact is
240 estimated to be minor.

241 **3.2. Biogeochemical properties and phytoplankton community**

242 **3.2.1. Expected biogeochemical properties of the resulting mixed waters**

243 The pH was very similar at the DCM and BEL at the OTEC site on D6 (8.24 and 8.25, respectively), whereas deep
244 seawater-pH showed lower value (7.81). The addition of 2 % and 10 % deep seawater to surface waters could thus induce a
245 pH-decrease of respectively, 0.01 and 0.07 unit. Hence, the effect on pH could be rather limited compared to the 0.1 pH
246 decrease (from 8.2 to 8.1) between the pre-industrial time and the 1990's (Orr et al., 2005).

247 NO_3^- and PO_4^{3-} concentrations (Table 3) were below the detection limit (< 0.02 μM) at the DCM (55 m) and BEL (80
248 m) at the OTEC site on observational D4 (June 16th 2014), whereas Si(OH)_4 concentrations were above detection limit
249 (> 0.08 μM), particularly at the DCM (2.4 μM). NO_2^- concentrations showed the highest values at the BEL whereas they
250 were negligible at the DCM (< 0.02 μM). In deep seawater, as commonly observed, NO_3^- , PO_4^{3-} and Si(OH)_4 concentrations
251 were largely higher compared to the surface (Table 3). The 2 % and 10 % deep water additions represented a large input
252 for NO_3^- in surface waters (from < 0.02 μM to 0.54 and 2.71 μM , respectively; Table 3). If the 10 % ratio also induced a large

253 input of PO_4^{3-} (from <0.02 to $0.19 \mu\text{M}$), the input of 2 % deep water was more limited ($0.04 \mu\text{M}$). The effect of 2 % or 10 %
254 deep seawater addition was more limited for $\text{Si}(\text{OH})_4$ relatively to NO_3^- and PO_4^{3-} input, yet it accounted for 50-63 %
255 increase for 10 % deep seawater addition (Table 3). Finally, because deep and DCM waters were NO_2^- depleted, the deep
256 seawater input did not modify the NO_2^- concentration at the DCM. At the BEL, NO_2^- concentration was higher and the 10
257 % addition slightly diluted NO_2^- at this depth.

258 Mn showed maximum concentrations in the surface layer on D4 at the OTEC site (Table 4) decreasing with depth as
259 observed close to the Lesser Antilles in the Atlantic Ocean (Mawji et al., 2015), but the measured surface concentrations
260 were particularly high, especially at the DCM. Fe that commonly dispatches hybrid distribution combining a nutrient-type
261 profile in surface waters and a scavenged-type distribution in deep waters (Bruland, 2003) also exhibited high surface
262 values, particularly at the DCM (Table 4). Cd, Zn, Co, Ni, and Cu dispatched nutrient-type profiles, whereas Pb exhibited
263 scavenged-type profile (Nozaki, 1997; Gruber, 2008), but like for dissolved Fe and Mn, their concentrations in the upper
264 waters were particularly high (Table 4). For all trace metals at both depths, the 2 % deep seawater addition will not induce
265 significant changes in their surface concentrations (Table 4). The 10 % deep seawater addition could increase Cd, Ni and Zn
266 concentrations in surface waters (Table 4), whereas it would not constitute an input of Pb, Cu, Co, and Fe, and it can even
267 dilute Mn (Table 4).

268 The surface waters can thus be enriched in macronutrients (NO_3^- , PO_4^{3-}) when submitted to a deep seawater
269 discharge (particularly with 10 % deep seawater addition) in proportion depending on the depth. The same scheme can be
270 applied in some of the dissolved trace metals (Cd, Ni, Zn) when a large ratio of deep seawater (10 %) is discharged.

271 3.2.2. Phytoplankton community in the natural environment

272 A set of seven accessory pigments identified as biomarkers of specific taxa (Uitz et al., 2010; Table 5) were analyzed
273 at OTEC station at D0, D4 and D6 in surrounding surface waters (Fig. 2), as well as population abundance and their
274 biovolume using light microscopy (Fig. 3).

275 TChl *a*, a proxy of the phytoplankton biomass, was higher at DCM than at BEL, as usually observed, by about two-
276 folds. The fucoxanthin (biomarker of diatoms) concentrations were similar at the DCM and BEL on D0 (Fig. 2), like the total
277 abundance of diatoms (Fig. 3). Fucoxanthin concentration increased by D4 and then by D6 at the DCM, corresponding to
278 increases of cumulated diatoms biovolume on D4 (Fig. 3) and of diatoms abundance on D6 (Fig. 3). Peridinin, a biomarker
279 of dinoflagellates, was detected at the DCM unlike at the BEL, with relatively high abundance and biovolume of
280 dinoflagellates (Fig. 3). The 19'-hexanoyloxyfucoxanthin (biomarker of haptophytes) concentration (Fig. 2) and the
281 prymnesiophytes (haptophyte) abundance and biovolume (Fig. 3) showed higher values at the DCM than at the BEL only
282 at D4.

283 At the DCM, dinoflagellates largely dominated the nano- and micro-phytoplankton assemblage with the largest
284 abundance and biovolume. Whereas prymnesiophytes showed the second highest abundance, its biovolume was very low,

285 on the contrary to diatoms that dispatched lower abundance but higher biovolume (Fig. 3). At the BEL, dinoflagellates,
286 prymnesiophytes and diatoms showed similar abundance, dinoflagellates and the diatoms occupied the major part of the
287 total biovolume. Three groups of dinoflagellates were observed by light microscopy but they could not be identified at
288 species level. However, their small size and the lack of colored starch (using lugol) in the cytoplasm suggested they were
289 mixotrophic or heterotrophic population. Furthermore, the low concentrations of peridinin in samples supported this
290 assumption.

291 At both depths, light microscopy analyses suggested that the large cyanobacteria, mainly *Trichodesmium*
292 *sp.*, were low in abundance and biovolume. Flow cytometry identification and count indicated that the small
293 cyanobacteria *Prochlorococcus* dominated the pico-phytoplankton assemblage, but they showed a significant
294 decrease from Do to D6 (Fig. 4). A significant portion of *Synechococcus* was also observed while picoeukaryotes
295 were poorly represented. Both *Prochlorococcus* and *Synechococcus* showed higher abundance at the DCM than at
296 the BEL (by 65 % and 86 %, respectively), in line with the pigment analyses of zeaxanthin (biomarker of
297 cyanobacteria) and total chlorophyll *b* concentrations (prochlorophytes).

298 3.2.3. Primary production and nitrate uptake in the natural environment

299 The phytoplankton distribution and assemblage can partly drive the intensity of primary production, so the specific
300 uptake rate of carbon (V_C ; Fig. 5) and NO_3^- ($V_{\text{NO}_3^-}$) were estimated at Do and D6.

301 V_C in surrounding surface waters was relatively low at Do (Fig. 5) indicating low primary production in these poor-
302 nutrients waters. Yet, V_C was approximately three-times higher at the DCM ($0.058 \mu\text{mol C} \cdot (\mu\text{g Chl } a)^{-1} \cdot \text{h}^{-1}$) than at the BEL
303 ($0.017 \mu\text{mol C} \cdot (\mu\text{g Chl } a)^{-1} \cdot \text{h}^{-1}$) at Do, but drastically decreasing on D6 at the DCM (to $\sim 0.014 \mu\text{mol C} \cdot (\mu\text{g Chl } a)^{-1} \cdot \text{h}^{-1}$). $V_{\text{NO}_3^-}$
304 were also very low at Do ($0.014 \mu\text{mol N} \cdot (\mu\text{g Chl } a)^{-1} \cdot \text{h}^{-1}$ at DCM, $0.017 \mu\text{mol N} \cdot (\mu\text{g Chl } a)^{-1} \cdot \text{h}^{-1}$ at BEL) and drastically
305 decreased at D6, below the detection limit (data not shown).

306 3.3. Impacts on the phytoplankton community of the deep seawater discharge

307 3.3.1. Changes in the phytoplankton assemblage

308 At the DCM, TChl *a* was similar in all treatments ($p < 0.05$) after 6 days of incubation in microcosms (Fig. 6). Only
309 fucoxanthin and 19'-butanoyloxyfucoxanthin showed significant ($p < 0.05$) higher concentrations in 10 % enrichments as
310 compared to controls, indicating higher abundance and/or biovolume of diatoms and haptophytes. The other diagnostic
311 pigments did not show any significant difference between enriched microcosms and controls. Picoeukaryotes and
312 *Synechococcus* abundances did not show significant variations between the treatments (Fig. 7a). Reversely,
313 *Prochlorococcus* population showed higher ($p < 0.05$) abundance both in 2 % and 10 % enriched microcosms as compared
314 to controls (Fig. 7a).

315 At the BEL, after the 6 days incubation period, pigments concentrations were below the detection limit indicating
316 very low abundance of phytoplankton. Pico-phytoplankton did not show significant variations between the treatments

317 and the controls (Fig. 7b). Pico-phytoplankton were clearly much less abundant at the BEL ($< 1000 \text{ cells.mL}^{-1}$) than at DCM
318 (Fig. 7b), 20-times even lower than that observed in surrounding waters at this depth on D6. For comparison, total
319 abundance at the DCM was ~ 5 -times lower in incubated microcosms on D6 compared to surrounding surface waters.

320 3.3.2. Changes in the primary production and nitrate uptake

321 Deep water inputs (2 % and 10 %) to surrounding waters collected at the DCM on D0 led to an increase of V_C within
322 24 h compared to the controls (by 42 % and 49 %, respectively; Fig. 5); but they had no effect on D6 despite very low value
323 in natural waters at this depth ($0.014 \mu\text{mol N} \cdot (\mu\text{g Chl } a)^{-1} \cdot \text{h}^{-1}$). The 6 days incubated microcosms showed very low V_C in all
324 treatments (Fig. 5). At the BEL, V_C were quite similar on D0 and D6 and after 6 days of incubation. V_C increased by 57% with
325 10% addition of deep water on D0 and was approximately two times higher than the control with the two enrichments on
326 D6 (Fig. 5). $V_{\text{NO}_3^-}$ measured in microcosms after a 6-days *in situ* incubation were below the detection limit (data not shown).

327 4. Discussion

328 4.1. Natural variabilities in the oligotrophic area

329 4.1.1. Biogeochemistry and phytoplankton community structure

330 The very low PO_4^{3-} and NO_3^- concentrations recorded in the oligotrophic surrounding surface waters were likely
331 favorable to the development of small phytoplankton, especially to the cyanobacteria as shown with the significant
332 occurrence of *Prochlorococcus* in these waters, which are typical of poor nutrient waters (Partensky et al., 1999). In line
333 with the very low $V_{\text{NO}_3^-}$ measured here, it has been shown that $V_{\text{NO}_3^-}$ by *Prochlorococcus* represents indeed only 5-10 % of its
334 nitrogen uptake whereas reduced nitrogen substrates (NO_2^- , ammonium, and urea) uptake accounts for more than 90-95
335 % (Casey et al., 2007). By contrast, the development of larger phytoplankton taxa (particularly diatoms), which have higher
336 NO_3^- and PO_4^{3-} requirements for their growth, were probably limited by these elements. Actually, NO_3^- and PO_4^{3-}
337 concentrations in surrounding waters at the DCM were both lower than the detection limit ($< 0.02 \mu\text{M}$ at D4) which is much
338 lower than the average values of half-saturation constants for diatoms ($1.6 \pm 1.9 \mu\text{M}$ for NO_3^- and $0.24 \pm 0.29 \mu\text{M}$ for PO_4^{3-} ;
339 Sarthou et al., 2005). For Si(OH)_4 , surrounding surface concentrations at DCM ($2.39 \mu\text{M}$) were in the range of diatoms half-
340 saturation constants ($3.9 \pm 5.0 \mu\text{M}$; Sarthou et al., 2005), hence the diatoms development was probably not limited by
341 Si(OH)_4 . Furthermore, diatoms showed low abundance in spite of relatively high Si(OH)_4 and dissolved trace metals (in
342 particular Fe) concentrations in surface waters. The potential of Fe limitation on phytoplankton community has been
343 reported previously in upwelling systems, with an apparent half-saturation constant for diatoms growth of 0.26 nM Fe in
344 the Peru Upwelling system (Hutchins et al., 2002). This constant is far lower than the concentration of Fe measured in
345 surrounding waters at DCM ($1.08 \pm 0.03 \mu\text{M}$ at D4), suggesting that diatoms were probably not limited by Fe. This further
346 supports growth limitation of diatoms by NO_3^- and/or PO_4^{3-} .

347 Advection of waters from Amazon and Orinoco rivers can explain the relatively high Si(OH)_4 observed in the
348 Caribbean Sea. However, little information is available on the input of trace metals by these waters into the Caribbean
349 Sea. Amazon river can be a source of dissolved Fe, Cu, Ni, Pb and Co for the western-subtropical North Atlantic (Tovar-
350 Sanchez and Sañudo-Wilhelmy, 2011), but this input can decrease rapidly away from its source like it has been shown for
351 Co in the Western Atlantic (Dulaquais et al., 2014). Those inputs into the Caribbean Sea will have to be further examined,
352 especially for Fe, Cd, Ni, Zn, Mn whose relatively high concentrations were detected in the Si(OH)_4 -enriched surface
353 waters of this study. Additionally, other inputs of trace metals such as atmospheric deposition can also increase surface
354 concentrations, and those inputs can be substantial (Shelley et al., 2012).

355 4.1.2. Primary production

356 Primary production rates measured in the oligotrophic surrounding waters were in the lower range of values
357 reported for oligotrophic waters (Laws et al., 2016; Teira et al., 2005). Despite low V_C on Do and D6 at the DCM, primary
358 production still indicated much higher value on Do compared to D6 that was associated with higher TChl *a* (Fig. 2a). The
359 decrease of divinyl-chlorophyll *a* concentration, a biomarker of *Prochlorococcus* (Goericke and Repeta, 1992), over the 6
360 days of observation can account for the decrease of TChl *a*, whereas chlorophyll *a* concentrations did not vary significantly
361 during this period. The *Prochlorococcus* abundance was also lower by two-times on D6 compared to Do (Fig. 4a). On the
362 contrary, fucoxanthin (diatoms) increased by four-times over the 6 days (Fig. 2a), as well as the diatoms abundance (by
363 three-times; Fig. 3a). In turn, the increase in diatoms abundance was not associated with an increase in primary
364 production. Instead, the observed decrease in primary production can be due to the decrease in *Prochlorococcus*
365 abundance. In tropical and subtropical waters, pico-phytoplankton can indeed contribute to more than 80 % of the primary
366 production (Platt et al., 1983; Goericke and Welschmeyer, 1993). The development of diatoms population likely did not
367 compensate the large decrease in *Prochlorococcus* abundance (from 141,000 to 63,000 cells.mL⁻¹).

368 4.2. Impact of deep seawater discharge

369 4.2.1. Temperature effects

370 The numerical simulation showed that the area impacted in the top-150 m by a temperature difference larger than or
371 equal to 0.3 °C (absolute value) was lower than 1 km² (~2-3 % of the considered domain) and was insensitive to the
372 injection depth or to the size of the tested domain (Table 2). The impact of a 0.3 °C temperature variation on the growth of
373 diatoms, notably on *Pseudonitzschia pseudodelicatissima* species that were observed in our study area, is limited to a
374 change in the growth rate of 0.03 d⁻¹ (Lundholm et al., 1997). For *Synechococcus*, a 0.3 °C variation of the temperature
375 would also have a limited impact on the growth, with a variation of only 0.02 d⁻¹ (Boyd et al., 2013), like for *Emiliania*
376 *huxleyi* (coccolithophyceae) for which the induced variation of maximum growth rate will be lower than 0.01 d⁻¹ (Fielding,
377 2013). The thermal effect on the phytoplankton assemblage could thus be considered negligible.

378 4.2.2. Impact on the phytoplankton community

379 Microcosms enrichment of DCM waters with 10 % of deep seawater led after 6 days to a significant increase
380 ($p < 0.05$) of fucoxanthin (diatoms) and 19'-butanoyloxyfucoxanthin (haptophytes) by 71 % and 77 %, respectively, as
381 compared to the controls. If the 2 % enrichment also showed similar trends, the differences of diagnostic pigments
382 concentrations were not significant. NO_3^- and PO_4^{3-} concentrations induced by 10 % deep-water input on D0 (2.57 ± 0.13
383 μM and $0.14 \pm 0.2 \mu\text{M}$, respectively; Giraud et al., 2016) were close to NO_3^- and PO_4^{3-} half-saturation constants of diatoms
384 ($1.6 \pm 1.9 \mu\text{M}$ and $0.24 \pm 0.29 \mu\text{M}$, respectively; Sarthou et al., 2005). The 10 % enrichment could thus support a
385 development of diatoms. On the contrary, NO_3^- and PO_4^{3-} enrichments induced by 2 % addition of deep-water were too
386 low ($0.57 \pm 0.02 \mu\text{M}$ and $0.04 \pm 0.00 \mu\text{M}$, respectively; Giraud et al., 2016) compared to these half-saturation constants to
387 support the diatoms development. Therefore, the diagnostic pigments suggested a significant response proportionally to
388 the amount of added deep seawater.

389 *Prochlorococcus* were also more abundant ($p < 0.05$) in 2 % and 10 % treatments as compared to the controls. This
390 lack of further *Prochlorococcus* population increase in 10 % treatments could be attributed to a higher grazing pressure by
391 haptophytes and/or to NO_3^- and PO_4^{3-} too rich conditions (Giraud et al., 2016).

392 Phytoplankton assemblage widely evolved in surrounding waters, from a predominance of pico-phytoplankton
393 (*Prochlorococcus*) on D0 towards a higher abundance of micro-phytoplankton (diatoms) on D6. In order to assess if the
394 impact on the phytoplankton assemblage due to 10 % deep seawater addition (with a shift towards the diatoms) was in
395 the range of the natural variation observed in the surrounding surface waters, 10 % deep seawater microcosms
396 phytoplankton assemblage was compared to the natural phytoplankton assemblage.

397 Whereas microcosm controls showed a lower *Prochlorococcus* abundance (Fig. 7a) than surrounding surface waters
398 on D6 ($p < 0.05$), the 10 % microcosms additionally showed, higher fucoxanthin (diatoms) and 19'-butanoyloxyfucoxanthin
399 (haptophytes) by about 142 % and 317 % (Fig. 6), respectively, as compared to natural waters at D6. Furthermore, 10 %
400 enrichments showed a fucoxanthin increase over the 6 days period by 3-times higher than in surrounding waters, whereas
401 controls only showed an increase by 1.5-times higher than in surrounding waters. Therefore, it can be concluded that the
402 10 % deep seawater enrichment induced higher variations of the phytoplankton assemblage than those observed from D0
403 to D6 in surrounding surface waters.

404 V_C were higher ($p < 0.05$) both in 2 % and 10 % enrichments on D0 as compared to controls, suggesting a positive
405 response of phytoplankton to the deep seawater addition. Conversely, there was no carbon-uptake rate difference
406 ($p < 0.05$) between controls and enriched waters (with 2 % and 10 % of deep seawater) at D6 with the 6 days incubated
407 microcosms, suggesting that the observed community modifications did not change the primary production. Indeed, the
408 phytoplankton community was quite similar in surrounding surface waters on D6 and in 6 days-incubated microcosm

409 controls. Thus, only the initial phytoplankton assemblage and initial primary production in surrounding surface waters
410 would influence the response of the phytoplankton community and its production.

411 At the BEL, after 6 days of incubation, deep seawater addition experiments clearly showed lower effects on the
412 phytoplankton community than at the DCM. Indeed, whereas significant differences ($p < 0.05$) between 10 % enrichments
413 and controls were observed in diagnostic pigments concentrations at the DCM, pigments concentrations were too low at
414 the BEL to be quantified. It can be suggested that the lower population and lower carbon uptake could be related to the
415 lowest light availability.

416 Overall, the phytoplankton response was proportional to the amount of added deep seawater. If the phytoplankton
417 assemblage significantly varied over time in the environment, the 10 % deep seawater enrichment showed larger
418 variations (for diatoms and haptophytes) than those observed in the natural environment. The DCM should be more
419 impacted than the BEL by the deep seawater discharge even with a large deep seawater input. On the other hand, the
420 impact on the primary production largely depended on the initial phytoplankton assemblage, which was quite variable
421 over time. The modification of the phytoplankton community to a deep seawater input could also be depending on the
422 initial phytoplankton community. For that, the microcosm experiments did not allow drawing a scenario over the long
423 term of the potential modifications of the primary production and the phytoplankton community associated to the deep
424 seawater discharge by an OTEC.

425 Finally, light microscopy analyses showed a large abundance of dinoflagellates at the DCM (between 9,240 and
426 20,400 cells.mL⁻¹ on D6 and D4; Fig. 3 a) which could be mixotrophic or heterotrophic and thus probably exert a grazing
427 pressure on the phytoplankton, particularly on the pico-phytoplankton (Liu et al., 2002). However, in this study, the
428 zooplankton larger than 200 μm and its potential control on the phytoplankton community were not considered and
429 should be examined in future studies.

430 5. Conclusion

431 Two complementary approaches were applied to study the potential effects of the deep seawater discharge of the
432 planned OTEC plant on the phytoplankton community in oligotrophic waters off Martinique.

433 Because the distribution and the development of phytoplankton are directly linked to the surface stratification, it is
434 important to assess the thermal effect of deep seawater by an OTEC plant. Modelling of the deep seawater discharge
435 showed that the thermal structure of the top 150 m of the water column on large and near-OTEC sections should be very
436 slightly impacted for the lowest considered temperature differences $|\Delta T| \geq 0.3$ °C. If World Bank Group prescriptions of not
437 exceeding a higher temperature difference of 3 °C are followed, the environmental perturbations potentially caused by the
438 operation of the OTEC should be considered negligible. The area where the 150 m-depth waters are impacted by the
439 lowest considered temperature differences $|\Delta T| \geq 0.3$ °C would not exceed 1 km² in a worst-case scenario.

440 The phytoplankton community and its production could be impacted by a large deep seawater input. Whereas pico-
441 phytoplankton currently largely dominates the phytoplankton assemblage, a ratio of 10 % of deep seawater in DCM
442 waters could induce a shift toward the diatoms and micro-phytoplankton. The ratio of 2 % of deep seawater in DCM
443 waters only showed significant higher *Prochlorococcus* abundance than controls, but the assemblage and the primary
444 production were not modified by this lower input. The stimulation of *Prochlorococcus* could be due to one or some of the
445 following causes: NO_3^- and/or PO_4^{3-} supply, trace metal supply, lowered pH (higher availability of dissolved inorganic
446 carbon). Since the lower impact on the phytoplankton assemblage was obtained at BEL, this depth can be recommended
447 for the discharge the deep seawater to exploit the OTEC plant.

448 Although significant, these results would have to be extended to larger temporal scale, and the phytoplankton
449 interactions with higher trophic levels (such as zooplankton) must be studied.

450 Because no environment standards on the deep seawater discharge effects are available yet, a rigorous monitoring of
451 the phytoplankton community, biogeochemical parameters distribution and of the water column stratification must be
452 established as soon as the OTEC is implemented and during its continuous functioning.

453 **Acknowledgements**

454 This work was supported by France Energies Marines and part of the IMPALA project. We would like to thank the Captains
455 and crew members of the "Pointe d'Enfer", and the scientists in the laboratory at the University of the French West Indies
456 and Guiana at Martinique; Dominique Marie (UPMC, Roscoff, France) and Christophe Lambert (LEMAR, France) for their
457 help with the flow cytometry, and Anne Donval (LEMAR, France) for the pigment analyses.

458

459

460 **References**

- 461 Agawin, N.S.R., Duarte, C.M., Agustí, S.: Nutrient and temperature control of the contribution of picoplankton to
462 phytoplankton biomass and production. *Limnology and Oceanography*, 45(8), 1891–1891, 2000.
- 463 Aminot, A., and Kérouel, R.: Dosage automatique des nutriments dans les eaux marines : méthodes en flux continu.
464 Ifremer Eds., Méthodes d'analyse en milieu marin, Quae, 2007.
- 465 Aure, J., Strand, O., Erga, S.R., Strohmeier, T.: Primary production enhancement by artificial upwelling in a western
466 Norwegian fjord, *Marine Ecology Progress Series*, 39–470 52, 2007.
- 467 Bakun, A.: Global climate change and intensification of coastal ocean upwelling, *Science*, 247(4939), 198–201, 1990.
- 468 Boyd, P. W., Jickells, T., Law, C. S., Blain, S., Boyle, E. A., Buesseler, K. O., et al.: Mesoscale iron enrichment experiments
469 1993-2005: Synthesis and future directions, *Science*, 315(5812), 612–617, 2007.
- 470 Boyd, P.W., Rynearson, T.A., Armstrong, E.A., Fu, F., Hayashi, K., Hu, Z. et al.: Marine phytoplankton temperature versus
471 growth responses from polar to tropical waters—outcome of a scientific community-wide study, *PLoS One*, 8(5), e63091,
472 2013.
- 473 Bruland, K. W., Rue, E. L., Smith, G. J.: Iron and macronutrients in California coastal upwelling regimes: Implications for
474 diatom blooms, *Limnology and Oceanography*, 46, 1661–1674, 2001.
- 475 Bruland, K.W.: Controls on trace metals in seawater, *The Oceans and Marine Geochemistry, Treatise on*
476 *Geochemistry*, 6, 23-47, 2003.
- 477 Brzezinski, M.A.: The Si:C:N ratio of marine diatoms. Interspecific variability and the effect of environmental variables,
478 *Journal of Phycology*, 21, 347–357, 1985.
- 479 Carr, M. E., and Kearns, E. J.: Production regimes in four Eastern Boundary Current systems, *Deep Sea Research Part II:*
480 *Topical Studies in Oceanography*, 50(22), 3199–3221, 2003.
- 481 Carton, J.A., and Giese, B.S.: A reanalysis of ocean climate using Simple Ocean Data Assimilation (SODA), *Monthly*
482 *Weather Review*, 136(8), 2999–3017, 2008.
- 483 Casey, J. R., Lomas, M.W., Mandecki, J., Walker, D.E.: Prochlorococcus contributes to new production in the Sargasso Sea
484 deep chlorophyll maximum. *Geophysical Research Letters*, 34(10), 2007.
- 485 Chavez, F.P., Toggweiler, J.R.: Physical estimates of global new production: the upwelling contribution. In: Summerhayes,
486 C.P., Emeis, K.C., Angel, M.V., Smith, R.L., Zeitzschel, B. (Eds.), *Upwelling in the Ocean: Modern Processes and Ancient*
487 *Records*. Wiley, 313–320, 1995.
- 488 De Baar, H. J., Boyd, P. W., Coale, K. H., Landry, M. R., Tsuda, A., et al.: Synthesis of iron fertilization experiments: from
489 the Iron Age in the age of enlightenment, *Journal of Geophysical Research: Oceans* (1978–2012), 110(C9), 2005.
- 490 Duarte, C.M., Agustí, S., Agawin, N.S.R.: Response of a Mediterranean phytoplankton community to increased nutrient
491 inputs: a mesocosm experiment, *Marine Ecology Progress Series*, 195, 61–70, 2000.

492 Dugdale, R.C., and Wilkerson, F.P.: The use of ^{15}N to measure nitrogen uptake in eutrophic oceans; experimental
493 considerations, *Limnology and Oceanography*, 31(4), 673–689, 1986.

494 Dulaquais, G., Boye, M., Rijkenberg, M.J.A., Carton, X.J.: Physical and remineralization processes govern the cobalt
495 distribution in the deep western Atlantic Ocean. *Biogeosciences*, 11(6), 1561–1580, 2014.

496 Dussart, B.M.: Les différentes catégories de plancton, *Hydrobiologia*, 26, 72–74, 1966.

497 Escaravage, V., Prins, T.C., Smaal, A.C., Peeters, J.C.H.: The response of phytoplankton communities to phosphorus input
498 reduction in mesocosm experiments, *Journal of Experimental Marine Biology and Ecology*, 198, 55–79, 1996.

499 Fernández, I., Raimbault, P., Garcia, N., Rimmelin, P., Caniaux, G.: An estimation of annual new production and carbon
500 fluxes in the northeast Atlantic Ocean during 2001, *Journal of Geophysical Research: Oceans* (1978–2012), 110(C7), C07S13,
501 2005.

502 Fielding, S.R.: *Emiliana huxleyi* specific growth rate dependence on temperature, *Limnol. & Oceanogr*, 58(2), 663–666,
503 2013.

504 Giraud, M. : Evaluation de l'impact potentiel d'un upwelling artificiel lié au fonctionnement d'une centrale à énergie
505 thermique des mers sur le phytoplancton, Doctorat de l'Université de Bretagne Occidentale, 150 p., 2016.

506 Giraud, M., Boye, M., Garçon, V., Donval, A., De La Broise, D.: Simulation of an artificial upwelling using immersed in situ
507 phytoplankton microcosms, *Journal of Experimental Marine Biology and Ecology*, 475, 80–88, 2016.

508 Goericke, R. and Welschmeyer, N.A.: The Marine Prochlorophyte *Prochlorococcus* Contributes Significantly to
509 Phytoplankton Biomass and Primary Production in the Sargasso Sea, *Deep Sea Research Part I: Oceanographic Research*
510 *Papers*, 40(11), 2283-2294, 1993.

511 Goericke, R., and Repeta, D.J.: The pigments of *Prochlorococcus marinus*: The presence of divinyl chlorophyll a and b in a
512 marine prochlorophyte. *Limnology and Oceanography*, 37, 425–433, 1992.

513 Gruber, N.: The marine nitrogen cycle: overview and challenges, *Nitrogen in the marine environment*, 1–50, 2008.

514 Handå, A., McClimans, T.A., Reitan, K.I., Knutsen, Ø., Tangen, K., Olsen, Y.: Artificial upwelling to stimulate growth of
515 non-toxic algae in a habitat for mussel farming, *Aquaculture Research*, 45, 1798–1809, 2014.

516 Harrison, W.G., Harris, L.R., Irwin, B.D.: The kinetics of nitrogen utilization in the oceanic mixed layer: Nitrate and
517 ammonium interactions at nanomolar concentrations, *Limnology and Oceanography*, 41(1), 16–32, 1996.

518 Hasle, G.R.: The inverted microscope method, In: Sournia, A. (Ed.), *Phytoplankton Manual*. UNESCO, Paris, 1988.

519 Hillebrand, H., Durselen, C.D., Kirchtel, D., Pollinger, U., Zohary, T.: Biovolume calculation for pelagic and benthic
520 microalgae, *Journal of Phycology*, 35, 403–424, 1999.

521 Hooker, S.B., Clementson, L., Thomas, C.S., Schlüter, L., Allerup, M., Ras, J., Claustre, H., et al.: NASA Tech. Memo.
522 2012-217503, NASA Goddard Space Flight Center, Greenbelt, Maryland, 2012.

523 Hutchins, D.A., Hare, C.E., Weaver, R.S., Zhang, Y., Firme, G.F., DiTullio, G.R., Alm, M.B., Riseman, S.F., Maucher,
524 J.M., Geesey, M.E., Trick, C.G., Smith, G.J., Rue, E.L., Conn, J., Bruland, K.W.: Phytoplankton iron limitation in the
525 Humboldt current and Peru upwelling, *Limnology and Oceanography*, 47, 997–1011, 2002.

526 International Finance Corporation (IFC): World Bank Group, Environmental, Health, and Safety Guidelines for Liquefied
527 Natural Gas (LNG) Facilities, 2007.

528 Kagaya, S., Maeba, E., Inoue, Y., Kamichatani, W., et al.: A solid phase extraction using a chelate resin immobilizing
529 carboxymethylated pentaethylenhexamine for separation and preconcentration of trace elements in water samples,
530 *Talanta*, 79(2), 146–152, 2009.

531 Kress, N., Thingstad, T.F., Pitta, P., Psarra, S., Tanaka, T., Zohary, T., Groom, S., Herut, B., Mantoura, R.F.C., Polychronaki,
532 T., Rassoulzadegan, F., Spyres G.: Effect of P and N addition to oligotrophic Eastern Mediterranean waters influenced by
533 near-shore waters: a microcosm experiment, *Deep Sea Research Part II: Topical Studies in Oceanography*, 52, 3054–3073,
534 2005.

535 Laws, E.A., Bidigare, R.R., Karl, D.M.: Enigmatic relationship between chlorophyll a concentrations and photosynthetic
536 rates at Station ALOHA, *Heliyon*, 2, e00156, 2016.

537 Liu, H., Suzuki, K., Saino, T.: Phytoplankton growth and microzooplankton grazing in the subarctic Pacific Ocean and the
538 Bering Sea during summer 1999, *Deep Sea Research Part I: Oceanographic Research Papers*, 49(2), 363–375, 2002.

539 Lundholm, N., Skov, J., Pocklington, R., Moestrup, Ø.: Studies on the marine planktonic diatom *Pseudo-nitzschia*. 2.
540 Autecology of *P. pseudodelicatissima* based on isolates from Danish coastal waters, *Phycologia*, 36(5), 381–388, 1997.

541 Marie, D., Partensky, F., Vaulot, D., Brussaard, C.: Enumeration of phytoplankton, bacteria, and viruses in marine samples,
542 *Current protocols in cytometry*, 1–11, 1999.

543 Mawji, E., Schlitzer, R., et al.: The GEOTRACES intermediate data product 2014, *Marine Chemistry*, 177(1), 1-8, 2015,
544 doi 10.1016/j.marchem.2015.04.005.

545 Milne, A., Landing, W., Bizimis, M., Morton, P.: Determination of Mn, Fe, Co, Ni, Cu, Zn, Cd and Pb in seawater using high
546 resolution magnetic sector inductively coupled mass spectrometry (HR-ICP-MS). *Analytica Chimica Acta*, 665(2), 200–207,
547 2010.

548 National Oceanic and Atmospheric Administration (NOAA): Ocean thermal energy conversion final environmental impact
549 statement. Office of Ocean Minerals and Energy, Charleston, SC, 1981.

550 National Oceanic and Atmospheric Administration (NOAA): Ocean thermal energy conversion: Assessing potential
551 physical, chemical, and biological impacts and risks. University of New Hampshire, Durham, NH, 2010.

552 Nozaki, Y.: A fresh look at element distribution in the North Pacific Ocean, *Eos Transaction*, 78(21), 221, 1997.

553 Orr, J.C., Fabry, V.J., Aumont, O., Bopp, L., Doney, S.C., Feely, R.A., Gnanadesikan, A., Gruber, N., Ishida, A., Joos, F., Key,
554 R.M., Lindsay, K., Maier-Reimer, E., Matear, R., Monfray, P., Mouchet, A., Najjar, R.G., Plattner, G.K., Rodgers, K.B., Sabine,

555 C.L., Sarmiento, J.L., Schlitzer, R., Slater, R.D., Totterdell, I.J., Weirig, M.F., Yamanaka, Y., Yool, A.: Anthropogenic ocean
556 acidification over the twenty-first century and its impact on calcifying organisms, *Nature*, 437(7059), 681–686, 2005.

557 Partensky, F., Hess, W.R., Vaulot, D.: *Prochlorococcus*, a marine photosynthetic prokaryote of global significance,
558 *Microbiology and Molecular Biology Reviews*, 63 (1), 106–127, 1999.

559 Pauly, D., and Christensen, V.: Primary production required to sustain global fisheries, *Nature*, 374(6519), 255–257, 1995.

560 Platt, T., Rao, D. S., Irwin, B.: Photosynthesis of picoplankton in the oligotrophic ocean, *Nature*, 301, 702–704, 1983.

561 Rocheleau, G., Hamrick, J., Church, M.: Modeling the Physical and Biochemical Influence of Ocean Thermal Energy
562 Conversion Plant Discharges into their Adjacent Waters, Final Technical Report, U.S. Department of Energy Award N° DE-
563 EE0003638, Makai Ocean Engineering, Inc., Kailua, Hawaii, 2012.

564 Sarthou, G., Timmermans, K.R., Blain, S., Tréguer, P.: Growth physiology and fate of diatoms in the ocean: a review,
565 *Journal of Sea Research*, 53(1), 25–42, 2005.

566 Shchepetkin, A.F., and McWilliams, J.C.: Correction and commentary for “Ocean forecasting in terrain-following
567 coordinates: Formulation and skill assessment of the regional ocean modeling system” by Haidvogel et al., *J. Comp. Phys.*,
568 227, 3595–3624, *Journal of Computational Physics*, 228(24), 8985–9000, 2009.

569 Shchepetkin, A.F., and McWilliams, J.C.: The regional oceanic modeling system (ROMS): a split-explicit, free-surface,
570 topography-following-coordinate oceanic model, *Ocean Modelling*, 9(4), 347–404, 2005.

571 Shelley, R. U., et al.: Controls on dissolved cobalt in surface waters of the Sargasso Sea: Comparisons with iron and
572 aluminum, *Global Biogeochem. Cycles*, 26(2), GB2020, doi:10.1029/2011GB004155, 2012.

573 Slawyk, G., Collos, Y., Auclair, J.C.: The use of the ¹³C and ¹⁵N isotopes for the simultaneous measurement of carbon and
574 nitrogen turnover rates in marine phytoplankton, *Limnology and Oceanography*, 22, 925–932, 1977.

575 Taguchi, S., Jones, D., Hirata, J.A., Laws, E.A.: Potential effect of ocean thermal energy conversion (OTEC) mixed
576 water on natural phytoplankton assemblages in Hawaiian waters. *Bulletin of Plankton Society of Japan*, 34(2), 125–
577 142, 1987.

578 Teira, E., Mouriño, B., Marañón, E., Pérez, V., Pazó, M.J., Serret P, de Armas, D., Escánez, J., Woodward, E.M.S.,
579 Fernández, E.: Variability of chlorophyll and primary production in the Eastern North Atlantic Subtropical Gyre:
580 potential factors affecting phytoplankton activity. *Deep-Sea Research I*, 52, 569–288, 2005.

581 Thomas, C.R.: *Identifying Marine Phytoplankton*. Academic Press, Inc. San Diego, California, 1996.

582 Tovar-Sanchez, A., and Sañudo-Wilhelmy, S.A.: Influence of the Amazon River on dissolved and intra-cellular metal
583 concentrations in *Trichodesmium* colonies along the western boundary of the sub-tropical North Atlantic Ocean,
584 *Biogeosciences*, 8, 217–225, 2011.

585 Uitz, J., Claustre, H., Gentili, B., Stramski, D.: Phytoplankton class-specific primary production in the world's oceans:
586 seasonal and interannual variability from satellite observations, *Global Biogeochemical Cycles*, 24(3), 2010.

587 Van Oostende, N., Dunne, J. P., Fawcett, S. E., Ward, B. B.: Phytoplankton succession explains size-partitioning of new
588 production following upwelling-induced blooms, *Journal of Marine Systems*, 148, 14–25, 2015.
589 WoRMS Editorial Board: World Register of Marine Species. Available from <http://www.marinespecies.org> at VLIZ.
590 Accessed 2019-06-21. doi:10.14284/170), 2019.
591

592 **Tables**

593 **Table 1-** Comparison of analyses of SAFe (Sampling and Analysis of iron) S and D2 reference samples
 594 (<http://www.geotraces.org/science/intercalibration>) between ID-ICPMS values (this study) and the consensus values. Our
 595 mean reagent blanks (based on all blank determinations) for dissolved Cd, Pb, Fe, Ni, Cu, Zn, Mn and Co, and detection
 596 limits of ID-ICPMS estimated as three times the standard deviation of the mean reagent blanks are also shown.

597

	Cd (pM)	Pb (pM)	Fe (nM)	Ni (nM)	Cu (nM)	Zn (nM)	Mn (nM)	Co (pM)
SAFe D2								
This study	948.83 ± 65.95	28.86 ± 4.44	0.898 ± 0.098	8.60 ± 0.36	2.15 ± 0.16	7.29 ± 0.27	0.40 ± 0.05	40.12 ± 3.88
Consensus values	986.00 ± 23.00	27.70 ± 1.50	0.933 ± 0.023	8.63 ± 0.25	2.28 ± 0.15	7.43 ± 0.25	0.35 ± 0.05	45.70 ± 2.90
n=	20	20	18	19	22	13	23	23
SAFe S								
This study	7.24 ± 1.57	48.42 ± 6.08	0.087 ± 0.025	2.56 ± 0.55	0.55 ± 0.06	0.07 ± 0.06	0.75 ± 0.05	2.85 ± 0.81
Consensus values	1.10 ± 0.30	48.00 ± 2.20	0.093 ± 0.008	2.28 ± 0.09	0.52 ± 0.05	0.07 ± 0.01	0.79 ± 0.06	4.80 ± 1.20
n=	25	27	15	25	30	10	27	28
Detection Limit	0.996	0.613	0.032	0.096	0.011	0.129	0.001	0.07
Blanks	0.716	1.809	0.061	0.040	0.019	0.129	0.003	0.32

598

599

600 **Table 2-** Area (km²) (average and root mean square) impacted in the top-150 m by a temperature difference $|\Delta T| \geq 0.3$ °C
 601 on two vertical sections centered on the OTEC, considering eight depths of deep seawater discharge (45, 80, 110, 140, 170,
 602 250, 350, 500 m) (Giraud, 2016).

Depth of deep water discharge	Annual mean		June	
	Large domain	Near-OTEC domain	Large domain	Near-OTEC domain
45 m	0.4 ± 0.4	0.0 ± 0.1	0.0	0.0
80 m	0.6 ± 0.7	0.1 ± 0.1	0.4	0.0
110 m	0.6 ± 0.5	0.0 ± 0.1	0.9	0.0
140 m	0.4 ± 0.5	0.1 ± 0.1	0.1	0.0
170 m	0.5 ± 0.8	0.0 ± 0.1	0.5	0.0
250 m	0.5 ± 0.7	0.1 ± 0.1	0.1	0.0
350 m	0.5 ± 0.5	0.1 ± 0.1	0.0	0.0
500 m	0.5 ± 0.5	0.1 ± 0.1	0.3	0.0

603
 604 **Table 3-** Nitrate, silicate, phosphate and nitrite concentrations on June 16th 2014 (D₄) at the deep chlorophyll maximum
 605 (DCM), at the bottom of the euphotic layer (BEL), and at the deep seawater pumping depth. Concentrations were
 606 measured at the OTEC site (0 % addition of deep waters) and calculated for 2 % and 10 % deep seawater additions.

Depth (m)	Deep seawater ratio	[NO ₃ ⁻] (μM)	[Si(OH) ₄] (μM)	[PO ₄ ³⁻] (μM)	[NO ₂ ⁻] (μM)
DCM	0 %	< 0.02	2.39	< 0.02	0.02
	2 %	0.54	2.88	0.04	0.02
	10 %	2.71	4.82	0.19	0.02
BEL	0 %	< 0.02	1.46	< 0.02	0.32
	2 %	0.54	1.96	0.04	0.32
	10 %	2.71	3.98	0.19	0.29
1100	100 %	27.11	26.69	1.87	<0.02

607
 608 **Table 4-** Concentrations of dissolved trace metals (in nM): Mn, Fe, Cd, Zn, Co, Ni, Cu, Pb measured on June 16th 2014 (D₄)
 609 at the OTEC site at the DCM, BEL and 1100 m (0 % addition of deep waters), and their calculated concentrations in the
 610 mixtures with 2 % and 10 % addition of deep water.

Depth (m)	Deep seawater	Mn (nM)	Fe (nM)	Cd (nM)	Zn (nM)	Co (nM)	Ni (nM)	Cu (nM)	Pb (nM)
-----------	---------------	---------	---------	---------	---------	---------	---------	---------	---------

ratio									
	0 %	2.97 ± 0.17	1.08 ± 0.03	0.03 ± 0.01	1.54 ± 0.04	0.05 ± 0.00	2.22 ± 0.10	1.70 ± 0.18	0.03 ± 0.00
DCM	2 %	2.92	1.08	0.04	1.56	0.05	2.29	1.70	0.03
	10 %	2.71	1.09	0.07	1.63	0.05	2.60	1.71	0.03
	0 %	1.65 ± 0.04	0.68 ± 0.03	0.03 ± 0.00	0.65 ± 0.03	0.03 ± 0.00	2.26 ± 0.17	1.14 ± 0.10	0.03 ± 0.00
BEL	2 %	1.63	0.69	0.04	0.68	0.03	2.34	1.15	0.03
	10 %	1.52	0.73	0.08	0.82	0.03	2.64	1.21	0.03
1100	100 %	0.34 ± 0.02	1.22 ± 0.05	0.45 ± 0.01	2.39 ± 0.07	0.06 ± 0.00	6.00 ± 0.13	1.80 ± 0.08	0.02 ± 0.00

611

612 **Table 5-** Definition of the diagnostic pigments used as phytoplankton biomarkers (taxonomic significance) and associated
613 phytoplankton size class (Uitz et al., 2010).

614

Diagnostic Pigments	Abbreviations	Taxonomic Significance	Phytoplankton Size Class
Fucoxanthin	Fuco	Diatoms	microplankton
Peridinin	Perid	Dinoflagellates	microplankton
19'-hexanoyloxyfucoxanthin	Hex-fuco	Haptophytes	nanoplankton
19'-butanoyloxyfucoxanthin	But-fuco	Pelagophytes and Haptophytes	nanoplankton
Alloxanthin	Allo	Cryptophytes	nanoplankton
chlorophyll <i>b</i> + divinyl chlorophyll <i>b</i>	TChl <i>b</i>	Cyanobacteria, Prochlorophytes	picoplankton
Zeaxanthin	Zea	Chlorophytes, Prochlorophytes	picoplankton

615

616

617

618 **Figure captions**

619 **Figure 1-** Bathymetry of the parent and child (grey rectangle) domains interpolated from the GINA data base with a zoom
620 on the near domain (black rectangle); the oblique white and black lines represent the large and small sections,
621 respectively, used for numerical simulations.

622
623 **Figure 2-** Pigment concentrations (from HPLC analysis) at the OTEC site at the DCM (a) and at the BEL (b), on June 12th
624 (D₀), 16th (D₄), 18th (D₆) 2014 (bars represent the standard deviation).

625
626 **Figure 3-** Abundance and biovolume of micro- and part of nano-phytoplankton at the OTEC site on June 12th (D₀), 16th
627 (D₄), 18th (D₆) 2014, at the DCM (a and c, respectively) and at the BEL (b and d, respectively) (bars represent the standard
628 deviation).

629
630 **Figure 4-** Abundance of pico-phytoplankton at the DCM (a) and at the BEL (b), on June 12th (D₀), 16th (D₄), 18th (D₆) 2014
631 (bars represent the standard deviation).

632
633 **Figure 5-** Specific carbon uptake rate ($\mu\text{mol} \cdot (\mu\text{g Chl } a)^{-1} \cdot \text{h}^{-1}$) at the DCM (a) and BEL (b) depths, on June 12th (D₀), and 18th
634 (D₆), and in 6 days incubated microcosms (D₆), for the three mixing conditions (0 %, 2 % and 10 % of deep seawater
635 additions) (for surrounding waters bars represent the standard deviation for 2 replicates).

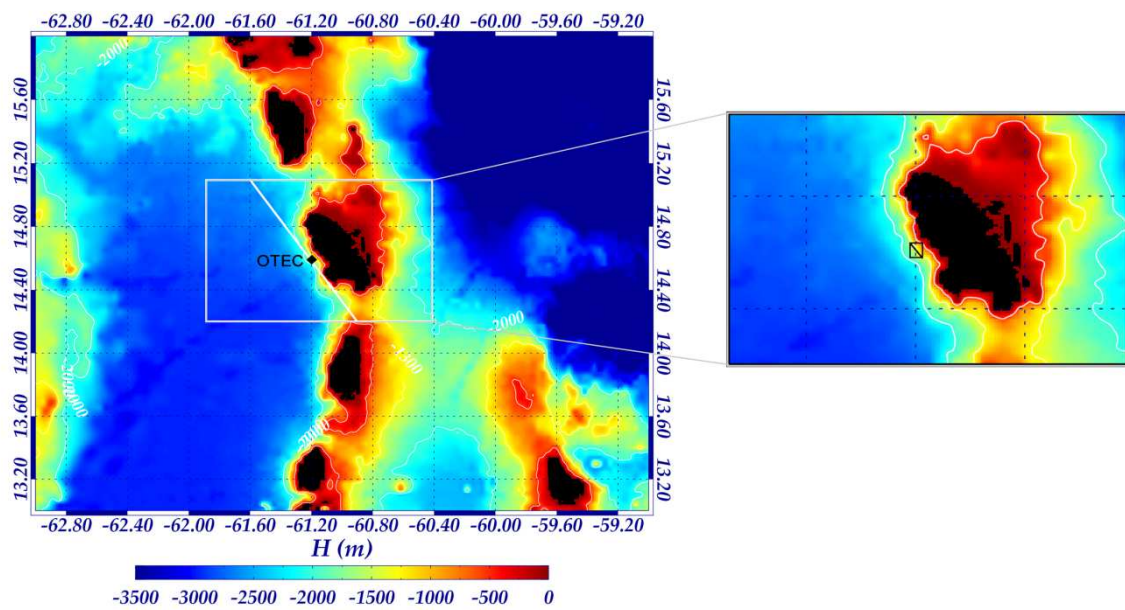
636
637 **Figure 6-** Diagnostic pigment concentrations in surrounding surface waters on D₀ and D₆, and in controls and deep water-
638 enriched (2 % and 10 %) microcosms after 6 days of incubation at the DCM (bars represent the standard deviation). Similar
639 letters (a, b or c) attributed to 2 or more treatments indicate no significant differences ($p < 0.05$) between these
640 treatments.

641
642 **Figure 7-** Abundance of picophytoplankton in surrounding surface waters on days 0 and 6, and in controls and deep water-
643 enriched (2 % and 10 %) microcosms after 6 days of incubation at 45 m depth (a) and 80 m depth (b) (bars represent the
644 standard deviation). Similar letters (a, b or c) attributed to 2 or more treatments indicate no significant differences ($p <$
645 0.05) between these treatments.

646
647
648
649

650 Figure 1

651



652

653

654

655

656

657

658

659

660

661

662

663

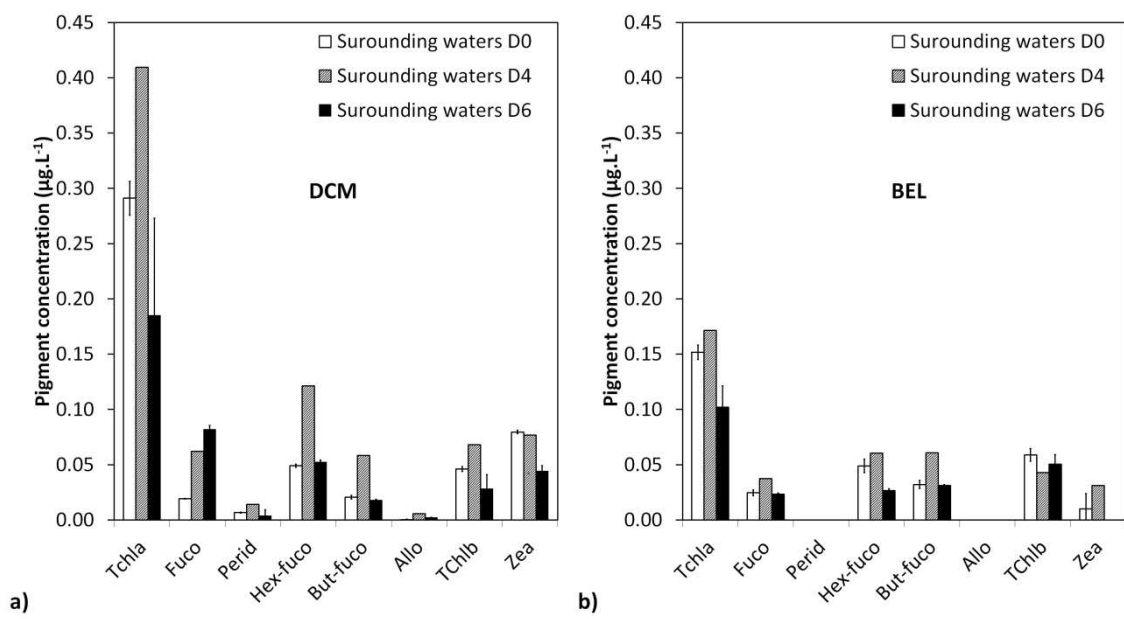
664

665

666

667 Figure 2

668



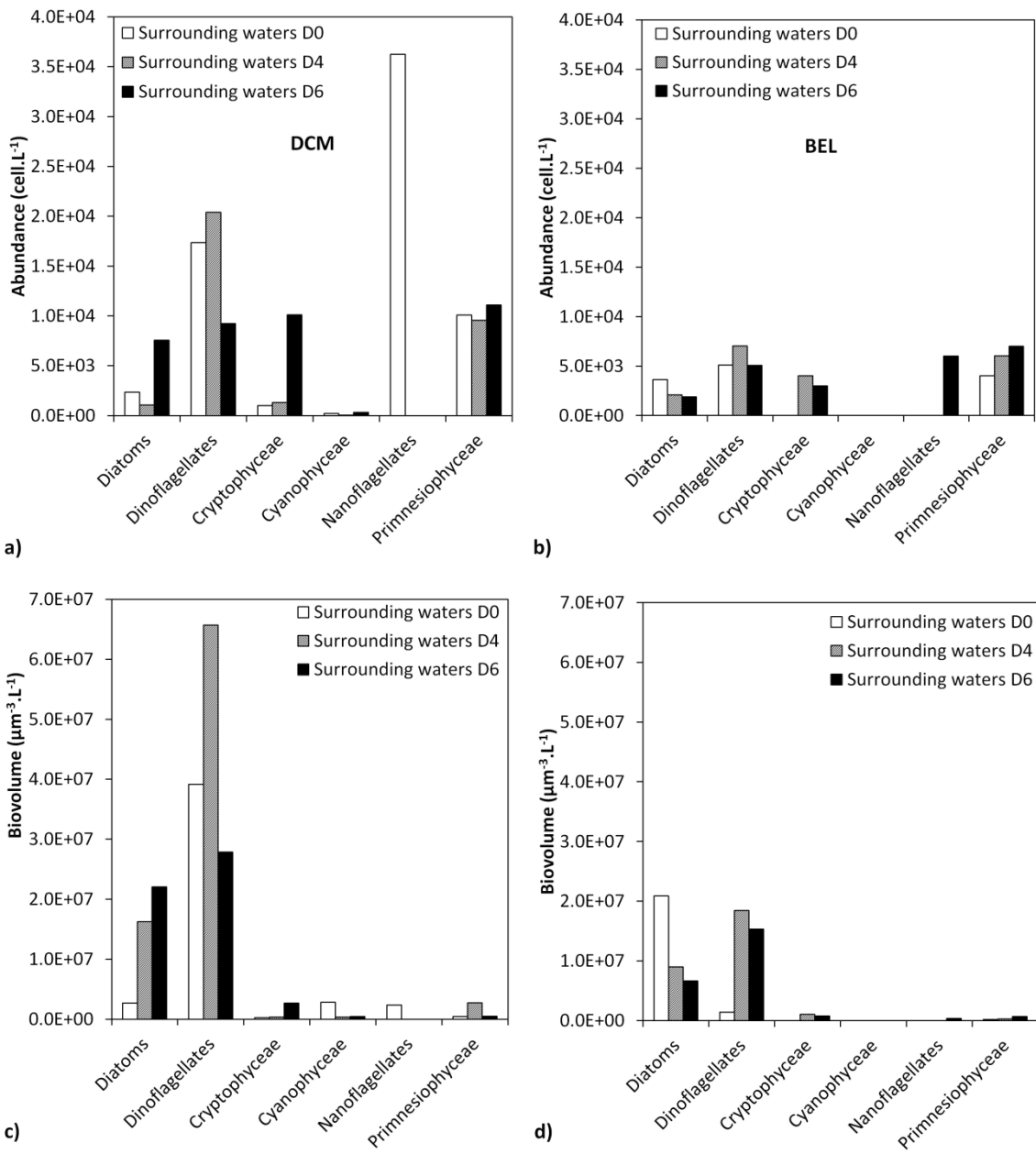
669

670

671

672

673 Figure 3



674

675

676

677

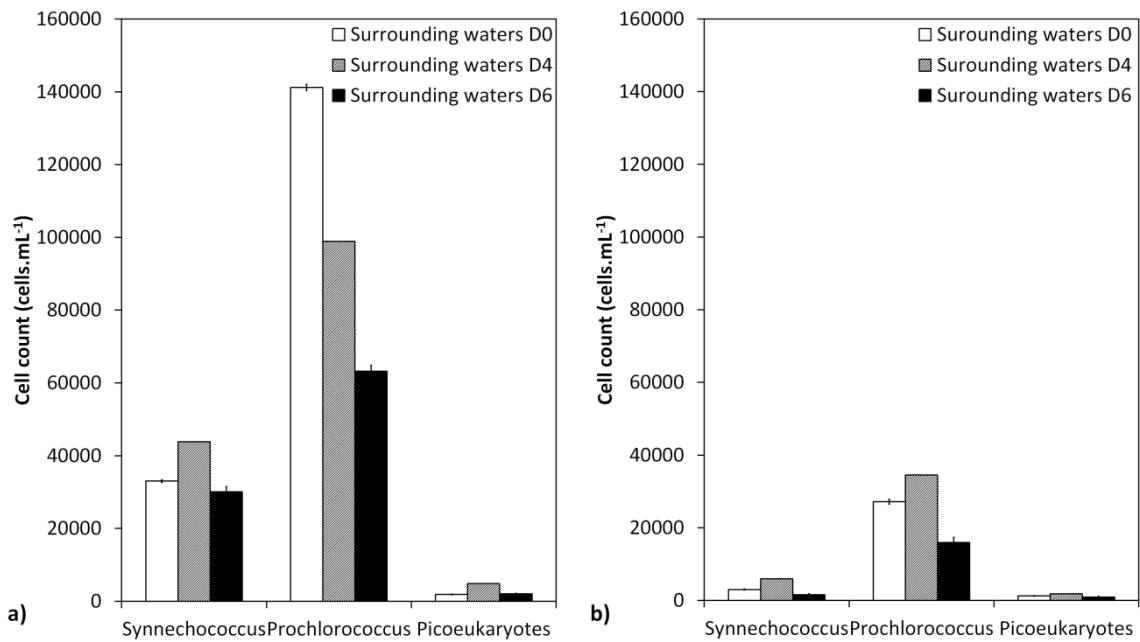
678

679

680

681 Figure 4

682

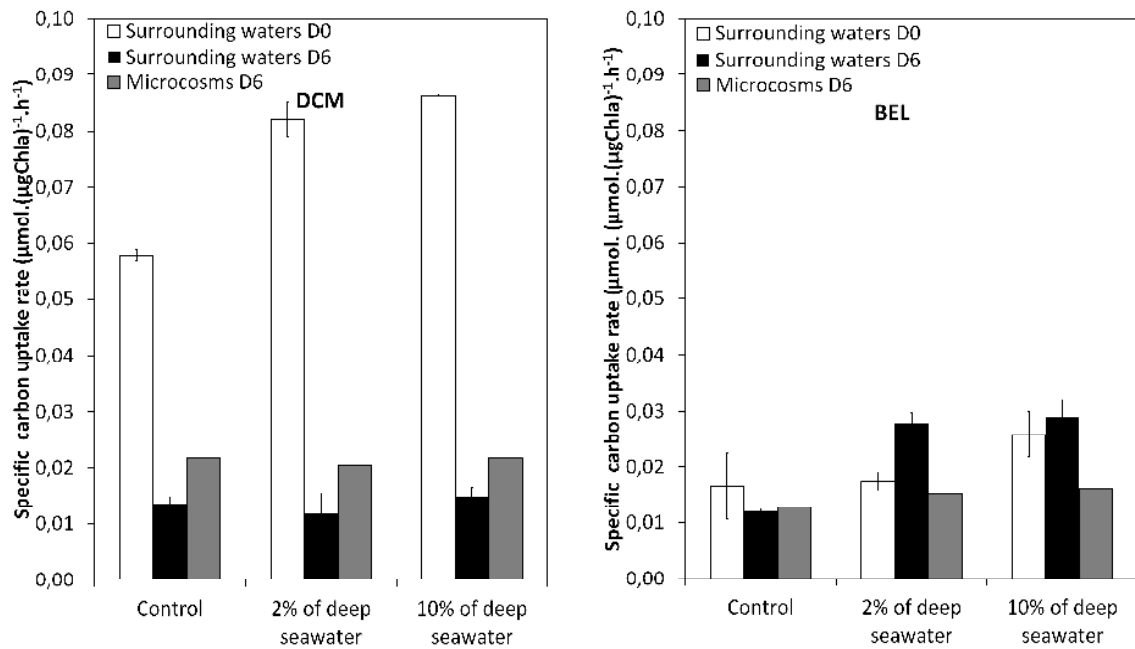


683

684

685

686 **Figure 5**



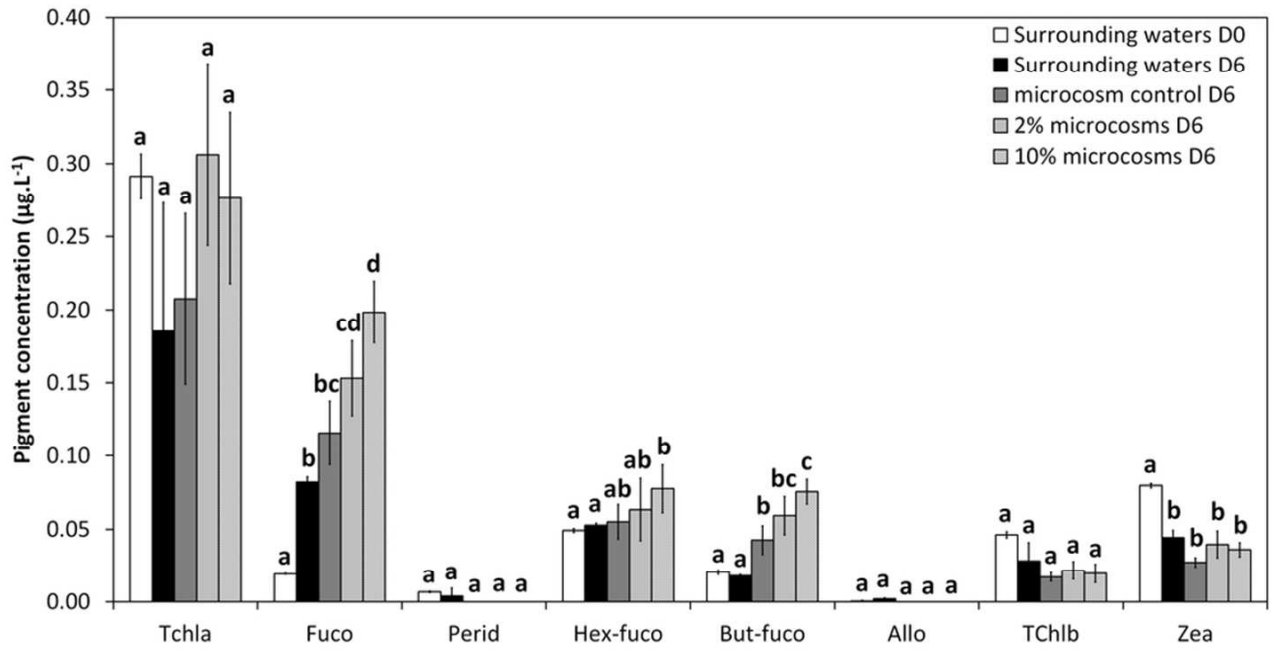
687

688

689

690 **Figure 6**

691



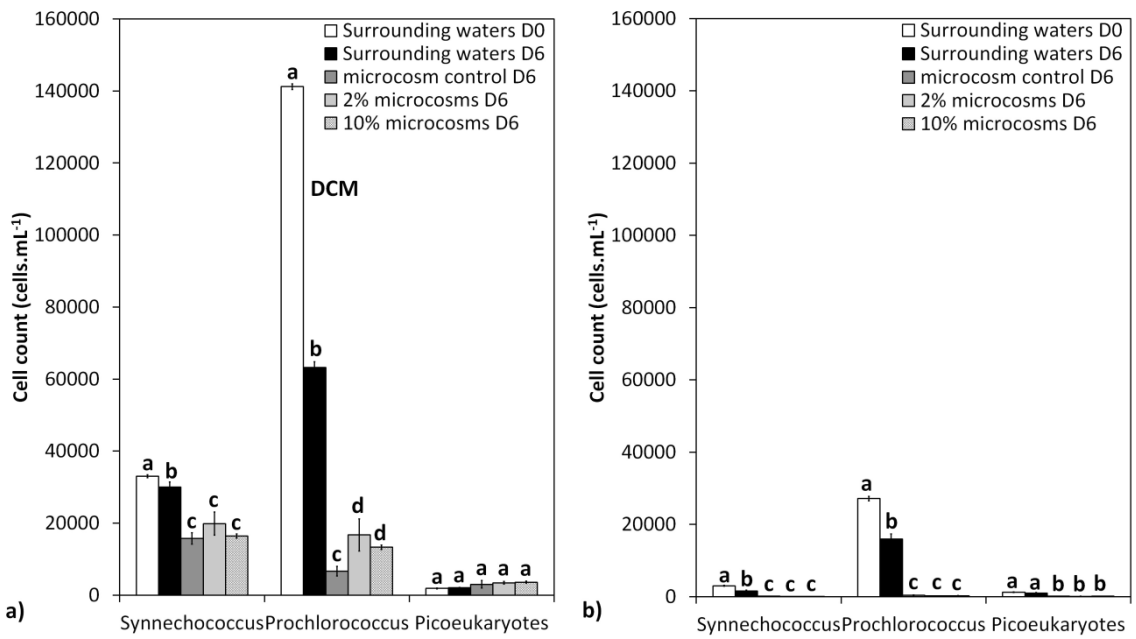
692

693

694

695 **Figure 7**

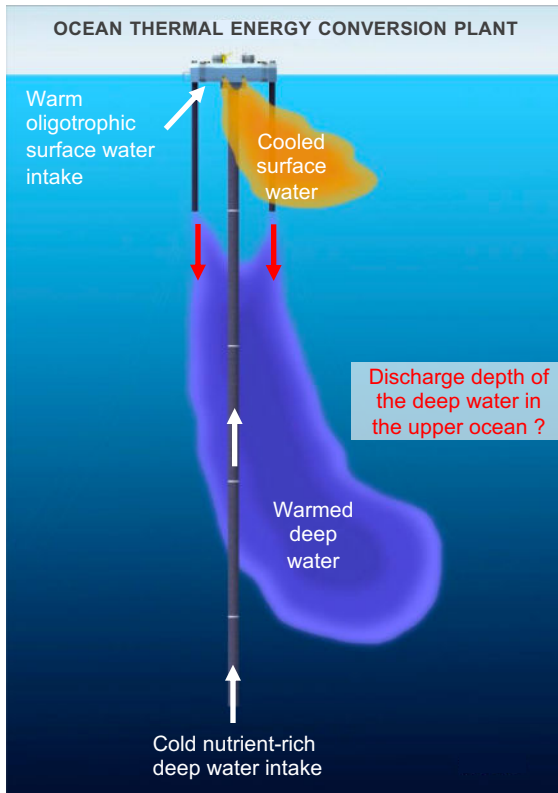
696



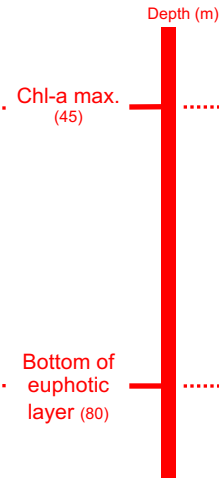
697

698

699



Modelling & Experimental microcosms



Effects on the phytoplankton assemblage

- **Thermal effect** : negligible ($\Delta T_{|0.3| \cdot C} < 1 \text{ km}^2$)
- **Biogeochemical effect** :
 - large shift of the assemblage with high deep water enrichment (10%)
 - limited effect with low deep water addition (2%)

- **Thermal effect** : negligible ($\Delta T_{|0.3| \cdot C} < 1 \text{ km}^2$)
- **Biogeochemical effect** : not significant → **Recommended depth for deep water discharge**